*33rd EPS Conference on Plasma Phys. Rome, 19 - 23 June 2006 ECA Vol.**30I**, P-1.098 (2006)*

Comparison of internal transport barrier evolution in MAST spherical tokamak plasmas with co- and counter-NBI heating

A. R. Field, R. J. Akers, N. J. Conway, A. Patel, M. J. Walsh
and the MAST and NBI teams

EURATOM/UKAEA Fusion Association, Culham Science Centre,
Abingdon, Oxon, OX14 3DB, UK

Introduction

Earlier studies of internal transport barrier (ITB) formation in MAST spherical tokamak plasmas compared transport properties between ITB discharges produced with co- and counter-current, tangential NBI heating [1-4]. Here results from similar discharges are presented where the ITB *evolution* is diagnosed using a new CXRS system [5] with unprecedented spatial resolution ($\Delta R \sim \rho_i$), providing full profiles of T_i and toroidal rotation ω_ϕ during the discharge at 5 ms intervals. The availability of only one NBI source, providing 1.6 MW (D^0), produces weaker, less broad ITBs than with the higher power from the two beams (2 MW, D^0 and H^0) available earlier. The availability of improved measurement data, combined with a newly developed integrated analysis chain [6], provides high-quality input data for transport analysis using TRANSP [7] and subsequent comparison of the results of transport analysis with theory and simulations. Here, for the first time, temperature gradients are compared with critical gradients for de-stabilisation of ITG, ETG and TEM micro-instabilities obtained from theoretical calculations [8, 9, 10].

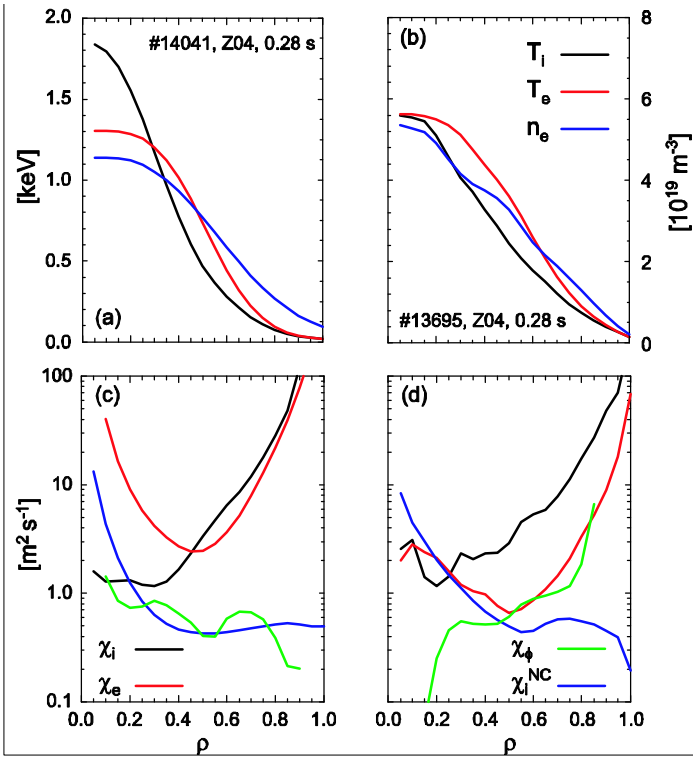

Fig. 1 (a) Profiles of T_e, T_i and n_e vs normalised radius ρ during ITB discharges with co- (#14041) and counter- (#13695) NBI heating at 0.28 s and (b) the corresponding thermal, χ_i, χ_e, and momentum, χ_ϕ, diffusivities from TRANSP analysis. The neo-classical ion thermal diffusivity χ_i^{NC} from NCLASS is shown for comparison.

ITB scenario

The ITB scenario is as used for the earlier studies [1] but with only 1.6 MW of NBI applied to a low-density target plasma from the beginning of a 4 MA/s current ramp up to a flat-top current of 800 kA. The density was constantly ramped during the sustained phase using outboard gas puffing. This and the unbalanced upper-DND magnetic configuration inhibits a transition to H-mode. There is significant absorption of the NBI power after ~ 0.1 s after which the stored energy W_{pl} increases throughout the discharges to the time of NBI cut-off at 0.3 s, to 80 kJ in the co-NBI case (#14041) and to 100 kJ in the counter-NBI case (#13695). That W_{pl} is higher with

counter- than with co-NBI heating is remarkable considering that the absorbed NBI power P_{abs} is much lower in the counter-NBI case (P_{abs}/P_{inj} ~ 30%) compared to the co-NBI case (~ 90%). The resulting thermal energy confinement time from TRANSP, $\tau_{E,th}$, is consequently about twice that in the counter- ($\tau_{E,th}$ ~ 80 ms) compared to the co- NBI case ($\tau_{E,th}$ ~ 40 ms), increasing throughout the discharge. In the co-NBI case Z_{eff}, determined from 2D images of the visible bremsstrahlung [11], is low (~ 1.2) over most of the profile rising in the boundary to ~ 2. In the counter-NBI case there is some impurity accumulation in the core with Z_{eff} peaking at ~ 2 and a strong increase in the boundary to ~ 4, possibly due to increased carbon sputtering from the prompt fast-ion losses.

Transport Analysis

Kinetic profiles from similar co- and counter-NBI ITB discharges are shown in Fig. 1 along with the corresponding transport coefficients at 0.28 s. In the co-NBI case, T_i exceeds T_e in the core and the T_i profile is more peaked. In the core (ρ < 0.4) the ion thermal diffusivity χ_i is within a factor of 2 of the neo-classical value χ_i^{NC} from NCLASS [12], indicating the presence of an ion ITB. In this region the E×B shearing rate ω_{SE} substantially exceeds an estimate of the linear ITG growth rate γ_m as shown in Fig. 3. In the core region χ_e exceeds χ_i, and outside (ρ > 0.4) both are equal and exceed χ_i^{NC} by an order of magnitude. The momentum diffusivity χ_ϕ is well below χ_i and is close to χ_i^{NC} over most of the profile. Fig 2 shows the evolution of the electron and ion pressure gradients $p'_{e,i}$ and ω_{SE}. In the co-NBI case the region of high ω_{SE}, which also corresponds to a region of low magnetic shear s ~ 0, is coincident with the maximum p'_i and evolves outwards from ρ ~ 0.2 to 0.4. In the counter-NBI discharge T_i ~ T_e and the profiles are broader than with co-NBI. Over most of the profile χ_e is lower than χ_i and inside ρ < 0.4 close to χ_i^{NC} indicating the presence of an electron ITB, whereas χ_i exceeds χ_i^{NC} by an order of magnitude. The p_e profile is broader than that of p_i and both are broader than in the co-NBI case. The E×B shearing rate ω_{SE} is also twice that in the co-NBI case and the profile is broader, increasing towards the plasma periphery. This is because, with counter-NBI the contributions to the radial E-field from V_ϕ and p'_i augment rather than oppose one another. Similarly to co-NBI the profiles of $p'_{i,e}$ and ω_{SE} broaden during the flat top phase from ρ ~ 0.3 to 0.7 to a larger radius than with co-NBI.

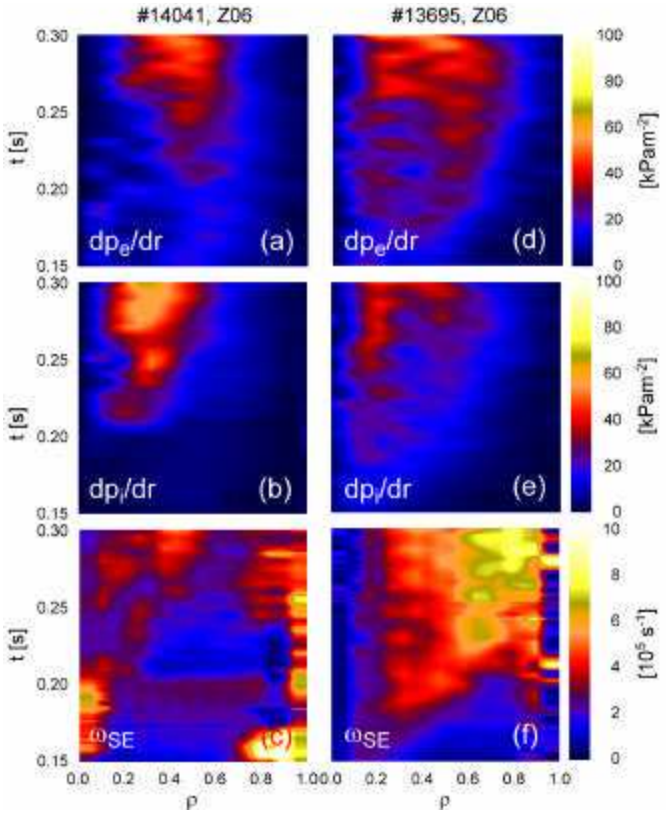

Fig. 2 Evolution of electron (a,d) and ion (b,e) pressure gradient and ExB shearing rate (c f) profiles for the co- (a,b,c) and counter- (d,e,f) NBI heated discharges shown in Fig 1.

Discussion

A critical ratio of the density and temperature gradient scale lengths, characterised by the parameter $\eta = L_n/L_T$ is required to linearly de-stabilise temperature gradient driven modes. This threshold behaviour can be understood in terms of the requirement for positive entropy production [13]. Fluid simulations indicate that sheared flows may shift the threshold gradients above the linear value [14]. Observed values of $\eta_{i,e}$ are compared in Fig. 4 with critical values predicted for ITG and ETG instabilities. Here expressions for these thresholds are used from Guo and Romanelli [8] for ITG modes:

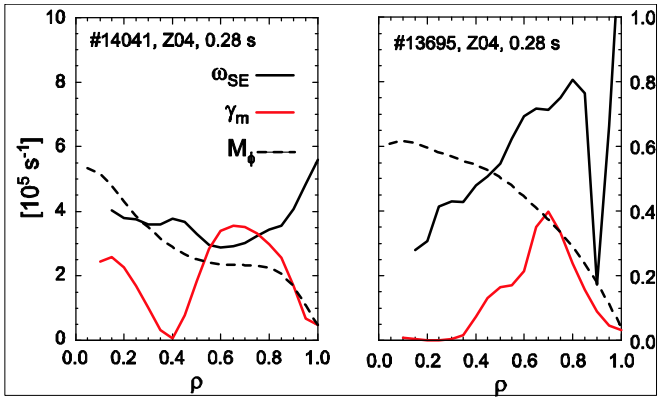

Fig. 3 Profiles of the E×B shearing rate ω_{SE}, the growth rate of the most unstable ITG mode γ_m, and the toroidal Mach number M_ϕ for the two discharges shown in Fig. 1.

$$\eta_{i,cr} = \max\left\{4/3(1+1/\tau)(1+2\hat{s}/q)\varepsilon_n, 1.2\right\} \quad (1)$$

where $\tau = T_e/T_i$ and $\varepsilon_n = L_n/R$, and from Jenko et al. [9] for ETG modes:

$$\eta_{e,cr} = \max\left\{(1+Z_{eff}\tau)(1.33+1.91\hat{s}/q)(1-1.5\varepsilon)(1+0.3\varepsilon(d\kappa/d\varepsilon))\varepsilon_n, 0.8\right\} \quad (2)$$

where $\varepsilon = r/R$ and k is the flux-surface elongation. These thresholds are obtained from linear, gyro-kinetic calculations at the ion and electron scales respectively. Note that, for both ITG and ETG modes there is a threshold ε_n above which the critical temperature gradient R/L_T is independent of the density gradient.

For the co-NBI discharge, in the region of reduced ion transport ($\rho < 0.5$) η_i exceeds the linear threshold value given by Equ. (1). Here, as show in Fig. 3, the prevailing ExB shearing rate ω_{SE} exceeds the estimated maximum growth rate γ_m of the ITG turbulence estimated from the analytic expression of Rogister [15], indicating that the sheared flow may have stabilised this branch of the turbulence. In contrast, in the outer region, where both the ion and electron anomalous transport is high, η_i is clamped close to the critical gradient whereas η_e exceeds that required to excite ETG turbulence, which may thus be driven into saturation [16]. Under such conditions, radially extended streamers can produce levels of electron transport at the levels observed. In this region ω_{SE} is comparable to the growth rate predicted for ITG modes, which hence may not be fully stabilised. In the case of the counter-NBI discharge, for both the ions and electrons the normalised gradients, $\eta_{i,e}$, are close to the threshold values. Over most of the profile χ_e is lower than χ_i and in the core region close to the ion neo-classical value, while the χ_i exceeds χ_i^{NC} over most of the

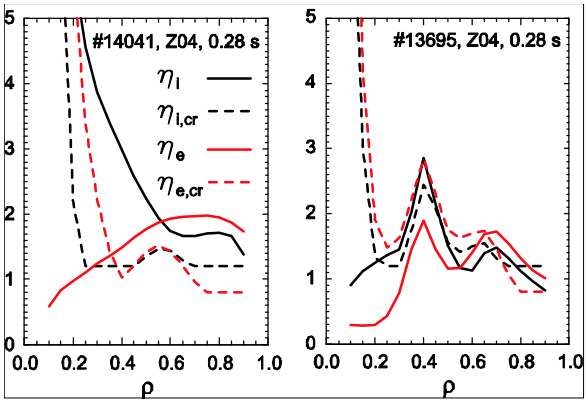

Fig. 4 Comparison of normalised ion and electron temperature gradients $\eta_{i,e}$ with critical values for the de-stabilisation of ITG and ETG micro-instabilities for the discharges shown in Fig. 1.

profile. This is remarkable considering that the shearing rate is almost twice that as in the co-NBI discharge, well exceeding the predicted ITG growth rate. A low level of electron thermal transport may be expected if the electron temperature gradient is close to the ETG turbulence threshold.

The earlier observation [1-4] of a very steep electron ITB at broad radius with higher power, counter-NBI heating prompted a theoretical study of the stability of TEM modes in the presence of a steep density gradient [10]. This study showed that collisional, dissipative TEM modes may be unstable if $\nu_e >> \varepsilon\omega$, where ν_e is the electron collision frequency and ω the mode frequency. In this case the stability of the modes is characterised by the parameter $\nu^*_{TEM} = \nu_e L_n / v_{th,i}$. Progressive stabilisation of the low-*k* part of the TEM spectrum is expected as $1/\nu^*_{TEM}$ exceeds 50. In the strong electron ITBs reported earlier stabilisation could be expected with $1/\nu^*_{TEM} \sim 60$ at the location of the ITB, which was co-incident with a local steepening of the density gradient. In the counter-NBI discharge discussed here there is no such localised electron ITB but rather a broad region of low electron transport. In this case the TEM stabilisation parameter $1/\nu^*_{TEM} \leq 20$ over the full profile so significant stabilisation is not expected. Recent gyro-kinetic studies of MAST plasmas indicate that there may be a significant drive from trapped particles in the intermediate-*k* region and thus TEM modes may play a role in the transport in these discharges [17].

Conclusions

The availability of high-resolution profile diagnostics has enabled the kinetic profile evolution of both the ions and electrons in co- and counter-NBI heated ST plasmas to be studied. Transport analysis indicates the formation of internal transport barriers in the plasma core, in the ion channel in the co- and electron channel in the counter-NBI cases. ITB formation is related to the prevailing high ExB shear and low magnetic shear. Comparison of the temperature gradients with estimates of thresholds for de-stabilisation of ITG and ETG modes indicates the presence of a degree of profile stiffness, except in the ion-ITB region where the threshold gradient is exceeded significantly as would be expected if there is suppression of anomalous transport.

References

[1] A.R. Field, R.J. Akers, L. Appel, 30th EPS CFPP Conference, St. Petersburg (2003) P2-148.
[2] A.R. Field, R. J. Akers, C. Brickley et al., 31st EPS CFPP Conf., London (2004) P4-187.
[3] A.R. Field, R.J. Akers, D. Applegate, 20th IAEA FEC, Vilamoura (2004) EX/4-4.
[4] H. Meyer, A. R. Field, R. J. Akers et al., Plasma Phys. Contr. Fus., **46** 5A (2004) A291-A298.
[5] N.J. Conway, P.G. Carolan, J. McCone et al., 16th APS Conf. HTPD (2006) Williamsburg.
[6] D. Muir, P.G. Carolan, R.J. Akers et al., 16th APS Conf. HTPD (2006) Williamsburg, USA.
[7] R.J. Hawryluk, in Proc. of Course in Physics to Thermonuclear Conditions, Varenna, (Commission of the European Communities, Brussels) Vol. I, (1980) 19.
[8] C.S. Guo, F. Romanelli, Phys. Fluids B, **5** (1993) 520.
[9] F. Jenko, W. Dorland, G. W. Hammett, Phys. Plasmas, **8** 9 (2001) 4096.
[10] J.W. Connor, R. J. Hastie, P. Helander, Plasma Phys. Contr. Fus., **48** 6 (2006) 885-900.
[11] A. Patel, P.G. Carolan, N.J. Conway, Rev. Sci. Inst. **75** 11 (2004) 4944-4950.
[11] W.A. Holberg et al., Phys. Plasmas, **4** (1997) 3230.
[12] W. Horton, G.T. Hoang, C. Bourdelle et al., Phys. Plasmas, **11** 5 (2004) 2600.
[13] A.M. Dimitz, B.I. Cohen, W.M. Nevins, Phys Plasmas, **7** (2000) 969.
[14] A.L. Rogister, Nucl. Fusion, **41** 8 (2001) 1101-1106.
[15] C.M. Roach, D. Applegate, J.W. Connor, Plasma Phys Contr Fus, **47** (2005) B323-B336.
[16] C.M. Roach, S. Saarelma, UKAEA Fusion, private communication.

This work was funded jointly by the United Kingdom Engineering and Physical Sciences Research Council and by the European Communities under the contract of Association between EURATOM and UKAEA. The views and opinions expressed herein do not necessarily reflect those of the European Commission.